Development of Functionally Graded Material through Friction Stir Processing

B.V. Himasekhar Sai

A Dissertation Submitted to

Indian Institute of Technology Hyderabad

In Partial Fulfillment of the Requirements for

The Degree of Master of Technology

Department of Mechanical and Aerospace Engineering

June, 2014

Declaration

I declare that this written submission represents my ideas in my own words, and where others' ideas or words have been included, I have adequately cited and referenced the original sources. I also declare that I have adhered to all principles of academic honesty and integrity and have not misrepresented or fabricated or falsified any idea/data/fact/source in my submission. I understand that any violation of the above will be a cause for disciplinary action by the Institute and can also evoke penal action from the sources that have thus not been properly cited, or from whom proper permission has not been taken when needed.

(Signature)

(B.V.Himasekhar Sai)

(ME12M1006)

ii

Approval Sheet

This thesis entitled – **Development of Functionally Graded Material through Friction Stir Processing** – by – B.V.Himasekhar Sai – is approved for the degree of Master of Technology from IIT Hyderabad.

Dr. M. Ramji
Department of Mechanical and Aerospace Engineering
IIT Hyderabad
Examiner

Dr. C. Viswanath
Department of Mechanical and Aerospace Engineering
IIT Hyderabad
Examiner

Dr. Abhay Sharma
Department of Mechanical and Aerospace Engineering
IIT Hyderabad
Adviser

Dr. S. Suriya Prakash
Department of Civil Engineering
IIT Hyderabad
Chairman

Acknowledgments

I would like to express my sincere thanks to my adviser **Dr. Abhay Sharma** for his constant support throughout my thesis work. His logical way of thinking and enthusiastic support motivated me a lot to do this project. The discussions that I had during group meetings with him were a major source of learning and improving my knowledge and communication skills. His guidance helped me all the time during the project.

I owe my sincere gratitude to **Dr. M. Ramji** for his valuable suggestions and support.

I would like to thank Department of Mechanical and Aerospace Engineering, IIT Hyderabad for providing all the necessary facilities during the research work.

I am grateful to **Saranath** and **Naresh** for sharing of knowledge and helping me a lot in my thesis work. I would like to thank my friends **Syed Quadir, Naveen, Somasekhara, Kishan, Nilanjan Banerjee** and **Jose M.J.** for their co-operation and generous help throughout my project. I would like to thank **Moulali Syed** and **Dhananjay Sahoo** for helping me in the manufacturing and metrology lab.

I would like to express my heartfelt thanks to all my classmates and my friends for giving me the moral support.

Dedicated to

My Parents

&

My Sisters

Contents

ABSTRACT

Functionally Graded Material (FGM) belongs to a new class of advanced material characterized by gradual variation in composition and the mechanical properties. The overall properties of the FGM are unique and different from the individual material used. Previous investigations show that various techniques such as powder metallurgy, centrifugal method, vapor deposition techniques, solid freeform fabrication methods and friction stir processing etc. have been used to fabricate the FGM. In order to overcome the control over the composition, the present study presents a method to fabricate functionally graded material using friction stir processing and hole drilling electrical discharge machine. Holes are drilled on an aluminum plate and filled with Alumina nano-particles of size (<50nm) and Titanium Carbide (TiC) particles of 325 mesh size and stirred using FSP. A mathematical model for positioning of holes in order to acquire a range of maximum to minimum composition of nano particles over a given length is presented. By aligning FSP tool center to hole center, multi-pass FSP is carried out in the same directions and in opposite directions to understand the material flow and mixing. SEM images and hardness analysis were used to evaluate the material flow and particle distribution. The strain variation along the longitudinal section parallel to the surface is measured. The mathematical model is applied to different combinations of composition ranges and is evaluated under different conditions.

List of Figures Page No.

List of Tables Page No.

Chapter - 1

Introduction

The concept of Functionally Graded Materials (FGMs) was founded by an organization “Functionally Graded Materials Forum, Japan” as a means of preparing thermal barrier materials. FGMs are a class of advanced materials of which the composition and mechanical properties change gradually from one side to the other. These materials can be designed for specific function and applications. Moreover, a graded change in material allows a reduction of stress concentrations appearing near a sharp interface between two different phases. Today, the FGM concept extends over a variety of sectors all across the world. FGMs have found their place in fields like bio-medical, automotive and aerospace, electronics, optics and nuclear applications, reactor and energy conversion. FGMs can be classified based on their applications such as (functionally graded joints, functionally graded coatings and functionally graded materials), according to their components (ceramics-ceramics, ceramics-metal, metal-metal etc.), by the nature of gradient (physical, chemical), by gradient distribution (one-, two- and three dimensional), and so on.

There are several techniques such as powder metallurgy, centrifugal method, vapor deposition, rapid prototyping that are currently used for producing FGMs. Vapor deposition techniques are generally applied for fabrication of functionally graded coatings. Although powder metallurgy can be utilized for producing bulk FGMs, the shapes and sizes are usually limited. Whereas Friction stir processing (FSP), a solid state processing technique that uses the same physical principle as Friction stir welding (FSW) has been recently investigated for composite manufacturing.

The FSP, a non-consumable joining technique which has a rotating tool with a pin and a shoulder plunges onto the surface and moves transversely along the path. The rotating tool impels the viscoplastic deformation at the interface between the tool and work piece, causing heat generation which softens the material without reaching the melting point as shown in Fig. 1. The material flow is stirred and forged under shoulder pressure during the process [1].

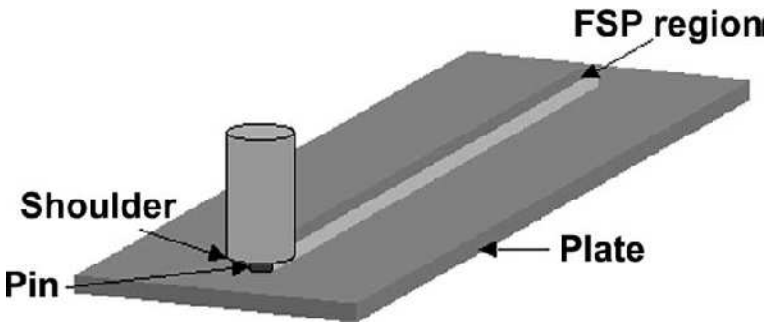

Fig. 1. A Schematic of the FSP [2]

Characteristics of Friction Stir Processing

1. Rotating tool pin and shoulder friction heats the contact faces. As the tool moves traverse, plasticized material is mechanically stirred and joined together.
2. Processing temperature occurs below the material melting point.
3. No toxic fumes and arc flashes.

The present study of fabrication of functionally graded material through Friction Stir Processing (FSP) is an attempt in order to overcome the control over the composition and the properties. Holes were drilled on an aluminium plate and filled with reinforcement particles. A mathematical model for positioning of holes has been developed in order to acquire the maximum to minimum composition of reinforcement particles over a given length.

Multi-pass FSP has been carried out in the same directions and in opposite directions by aligning the FSP tool center to hole center to understand the material flow and mixing at the longitudinal center along the direction parallel to the surface.

The strain measurement at the center of FGM along the longitudinal direction parallel to the surface was done using the Digital Image Correlation (DIC) technique. DIC is a non-contact optical technique used for measuring strain and displacement in components over a wide range of length scales. It is now being used extensively in experimental mechanics in a diverse range of applications like zone wise local characterization of welds, material characterization and deformation of large structures, high temperature strain mapping, crack tip and crack propagation studies. This technique suited for the characterization of material properties both in the elastic and plastic ranges. This technique is based on recording a series of images of the specimen during the deformation with digital cameras and calculating the

surface displacements from these images. In the present study 2D strain analysis was carried out using only one camera.

Organization of Thesis

In *chapter 1* an introduction to the report is presented. It starts with emphasizing on what is functionally graded material and friction stir processing.

In *chapter 2* literature survey of various approaches to fabricate the functionally graded material and objectives of the present study are discussed.

In *chapter 3* a mathematical model for positioning of holes in order to acquire the maximum to minimum composition of reinforcement particles over a given length is discussed.

In *chapter 4* the materials, the tool used, experimental method and the measurement techniques used to understand the material flow is described.

In *chapter 5* the results obtained by multi-pass FSP and the effect of multi-pass FSP on the material flow during the process is discussed.

In *chapter 6* conclusions and future scope is discussed.

Chapter - 2

Literature Survey

2.1 Literature Survey

From the previous investigations there are different kinds of processes to fabricate FGM using gases, liquids and solids as the starting materials such as powder metallurgy method, rapid prototyping technique, centrifugal method, vapor deposition technique, friction stir processing [3, 4].

2.1.1 Powder metallurgy method

Powder metallurgy method is used to produce the functionally graded material through three basic steps i.e. mixing of powders, stacking and ramming of the pre-mixed powders and finally sintering. Powder metallurgy method is known to be a cost efficient technique used to produce bulk FGM. Complex structures can be developed with more than two components but powder metallurgy technique gives rise in stepwise structure.

Zhu et. al [5] developed the ZrO_2–NiCr functionally graded material by powder metallurgical process and also demonstrated the chemical composition and microstructure distribution in stepwise which improved the mechanical properties.

Gang Jin et. al [6] developed the Mullite/Mo functionally graded material by powder metallurgy process. Thermo mechanical properties of Mullite/Mo FGM are compared with the monolithic Mullite, where FGM has the better properties over the monolithic Mullite.

Zhang et. al [7] fabricated the bulk SiC/C FGM with different number of graded layers by powder stacking method and studied the effect of number of graded layers on microstructure and properties of SiC/C FGM. It was observed that with increase in the number of graded layers the interface between the layers faded away resulting in linearly continuous gradient of higher strength.

Bhattacharyya et. al [8] developed the multilayered Al/SiC FGM by the powder metallurgy process and the Ni/Al_2O_3 by the thermal spray technique and studied the microstructure, porosity content and the properties like flexural strength, thermal fatigue behavior in which

as the number of layers increases from two to five keeping the extreme layers same, the considerable performance in FGM has been observed.

2.1.2 Centrifugal method

Centrifugal method is similar to centrifugal casting to produce bulk functionally graded material by spinning of the mould. If continuous structure is preferred then centrifugal method is used. Centrifugal method is limited to circular shapes and type of gradient produced since the gradient is formed through the natural process (centrifugal force and density difference).

Lai et. al [9] investigated the feasibility of FGM formation through centrifugally assisted combustion synthesis by choosing the thermite reactions and obtained the graded composition for a particular composition of copper in the thermite reaction.

Watanabe et. al [10] developed the metal-ceramic FGM with a mixture of plaster and corundum particles and studied the process parameters along with numerical model simulation. The simulation results gave results which matches with the experiments and shown that the composition gradient can be controlled by the mixture of particle sizes.

Zhai et. al [11] prepared aluminium based (Al-Si & Al-Si-Mg) functionally gradient composite tubes and compared their structural and mechanical properties from which gradual gradient in primary Si particles is observed in Al-Si tube in both the inner and the outer layers whereas in Ai-Si-Mg tube sudden change is observed and the hardness and wear resistance of inner layer in Al-Si-Mg tube is greater than the other layers of Al-Si-Mg tube and Al-Si tube (inner and outer layers) and found that the Mg_2Si formed in the process is the key aspect for these change.

2.1.3 Rapid prototyping technique

Rapid prototyping technique is an additive manufacturing process by which functionally graded material can be fabricated in higher production. This process has ability to design and produce complex shapes due to the liberty provided, as parts are developed directly from CAD data. This method provides manufacturing flexibility but characterized by poor surface finish followed by a secondary finishing operation.

Zhang et. al [12] developed the TiC-Ni FGM by the Laminated Object Manufacturing (LOM), a rapid prototyping technique and analyzed micro and phases with SEM and XRD and observed the anisotropic mechanical properties i.e. stronger in the direction of thickness than its perpendicular direction and the maximum strength and the highest density were observed in the TiC – 20wt.%Ni region.

Tao et. al [13] proposed a rapid prototyping manufacturing technology for glass-alumina functionally graded material based on the solidification of wax and observed the homogeneous distribution of ingredient materials and the bending strength increases with increase in content of alumina.

2.1.4 Vapor deposition technique

Vapor deposition methods are used to produce functionally graded surface coatings. This technique includes chemical vapor deposition and physical vapor deposition. These vapor deposition methods are used for depositing the thin surface coating by continuously changing the ratios of reactions in the starting mixture.

Kawase et. al [14] developed the SiC-C/C FGM by thermal-gradient chemical vapor infiltration of carbon followed by chemical vapor deposition of the SiC-C compositionally gradient layer changing the reactant mixture composition gradually from the propane to dimethyldichlorosilane and observed no thermal cracks.

2.1.5 Friction stir processing

Gandra et. al [15] produced aluminium based functionally graded metal matrix composite with a groove in which SiC ceramic particles with different median sizes followed by FSP and obtained orthogonal gradients of composition and mechanical behavior and observed that when the particles are compacted in a groove placed under the probe is more effective and small particles lead to higher along bead surface and to smooth fraction gradients both in and along the direction parallel to the surface. Hardness and particle fraction area are high at surface and at retreating side.

Kwon Yong-jai et. al [16] investigated the friction stir welding of 5052 aluminium plates at different rotation speed under a constant traverse speed and studied the surface appearance which is smooth at medium speeds and macro and micro

structures and investigated the mechanical properties hardness, tensile strength and observed they were high at low rotation speeds.

Uygur et. al [17] carried out the friction stir welding process on commercially pure aluminium with different shoulder diameters and studied the influence of shoulder diameter on temperature distribution, microstructure, hardness and tensile strength which gives good results at minimum shoulder diameters.

Palanivel et. al [18] studied the effect of tool rotation speed and pin profile on the microstructure and the tensile strength of dissimilar friction welded aluminium alloys and observed three different regions unmixed, mechanically mixed and mixed flow regions in the weld zone.

2.2 Objectives of present study

Considering the past work carried out in the study of fabrication of functionally graded materials, the present work explores the other aspects which include:

1. Developing a mathematical model for 1-dimensional functionally graded material with a linear change in composition of nano-particles under different conditions.
2. Predicting the effect of multi-pass FSP in the same directions and in opposite directions with a cylindrical pin tool on material flow.

Chapter – 3

Numerical Model

A mathematical model is needed to be formulated to optimally design various process parameters. This chapter describes the process description and the mathematical model. The process parameters include composition of reinforcement particles (maximum composition C_{max} and minimum composition C_{min}), Length of the grid (Δx_i), hole diameter (d), No. of holes (i) and FSP tool pin diameter (P_d).

3.1 Process description

In the present study, the functionally graded material is fabricated through FSP. In order to get the composition variation in the material, holes were drilled on an aluminium plate using hole electrical discharge machine and filled with reinforcement particles (Alumina and TiC). A mathematical model for positioning of holes has been developed in order to acquire the maximum to minimum composition of reinforcement particles over a given length.

After filling the particles in the holes, the material is allowed to dry. The process has been carried out on vertical milling machine with the FSP tool. By aligning the FSP tool center to hole center, the FSP tool pin is inserted into the predrilled hole (away from the particle holes) and on the filled holes, multi-pass FSP has been carried out in the same directions and in opposite directions as shown in Fig. 2. The FSP process has been carried with a tool rotation speed of 1000 rpm and the tool traverse speed of 50 mm/min.

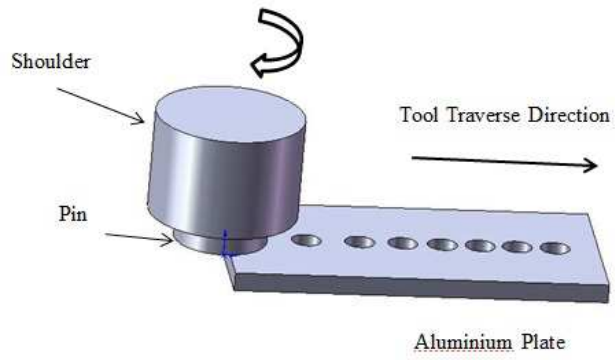

Fig. 2. FSP process on reinforcement particles

3.2 Process calculations

A mathematical model for the linear change in composition of functionally graded material has been presented with process parameters such as composition of reinforcement particles (maximum composition C_{max} and minimum composition C_{min}), Length of the grid (Δx_i), hole diameter (d), No. of holes (i) and FSP tool pin diameter (P_d). The composition change of reinforcement particles from C_{max} to C_{min} has been achieved linearly variation as follows

Assuming a grid of $\Delta x_i \times P_d$ as shown in Fig. 3

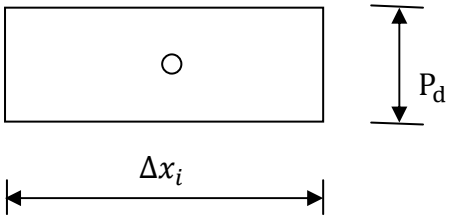

Fig. 3. Grid size

Where P_d - Pin diameter; Δx_i- Length of the grid.

In the present study, the composition of reinforcement particles is measured as ratio of volume of hole to grid (volume fraction of hole and grid).

The percentage volume fraction is defined as

$$C_i = \frac{\pi d^2 \times 100 \times P_l}{4 \times \Delta x_i \times P_d \times P_l} \quad (1)$$

Where d - Diameter of hole; C_i – percentage Composition; P_d- Pin diameter; x_i - Length of the grid;

P_l - Pin length.

In this mathematical model, the composition variation is assumed to be linearly changing with respect to the length as $C_i = b - ax_i$

Where $C_i = \frac{\pi d^2 \times 100 \times P_l}{4 \times \Delta x_i \times P_d \times P_l}$ (From Eq. (1))

$$b = C_{max} \quad (2)$$

$$a = \frac{C_{max} - C_{min}}{l} \quad (3)$$

Substituting Eqns (1), (2) & (3) lead to Eq. (4)

$$C_i = C_{max} - \left(\frac{C_{max} - C_{min}}{l}\right) x_i \tag{4}$$

i.e. $$\frac{\pi d^2 \times 100 \times P_l}{4 \times \Delta x_i \times P_d \times P_l} = C_{max} - \left(\frac{C_{max} - C_{min}}{l}\right) x_i \tag{5}$$

$$\frac{k}{\Delta x_i} = C_{max} - H \times x_i \tag{6}$$

Where $k = \frac{\pi d^2 \times 100 \times P_l}{4 \times P_d \times P_l}$

$H = \frac{C_{max} - C_{min}}{l}$

The two consecutive holes positioning (i and i+1) having lengths x_i and x_{i+1} from one end has been shown in Fig. 4 with the change in length of the grids. From the Fig. 4

$$x_{i+1} - x_i = \frac{\Delta x_i}{2} + \frac{\Delta x_{i+1}}{2} \tag{7}$$

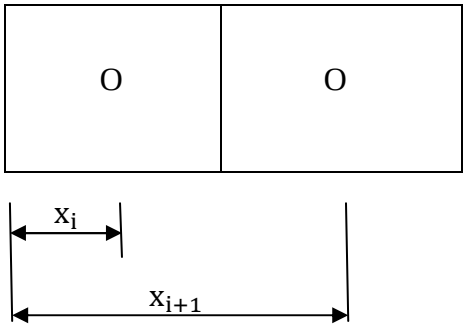

Fig. 4. x_i and x_{i+1} values

Here $C_{max} = \frac{\pi \times d^2 \times 100}{4 \times d \times P_d}$ (8)

Therefore,

$$C_{i+1} - C_i = a\,(\Delta x_{i+1} + \Delta x_i)/2 \tag{9}$$

$$\frac{k}{\Delta x_{i+1}} - \frac{k}{\Delta x_i} = a\,(\Delta x_{i+1} + \Delta x_i)/2 \tag{10}$$

$$\frac{2k}{a} \times \left(\frac{\Delta x_i - \Delta x_{i+1}}{\Delta x_i * \Delta x_{i+1}}\right) = \Delta x_{i+1} + \Delta x_i \tag{11}$$

$$\Delta x_i \times \Delta {x_{i+1}}^2 + \left(\Delta {x_i}^2 - \frac{2k}{a}\right) \times \Delta x_{i+1} + \frac{2k}{a} \times \Delta x_i = 0 \quad (12)$$

Let $f = \Delta {x_i}^2 - \frac{2k}{a}$

$g = \frac{2k}{a}$

Solving the Eq. (12) for Δx_{i+1} lead to Eq. 13

$$\Delta x_{i+1} = \frac{-f \pm \sqrt{(f^2 - 4 \times \Delta x_i \times g)}}{2 \times \Delta x_i} \quad (13)$$

These values are calculated up to Δx_{i+1} reaches the value of total calculated length L_i

$$L_i = \sum \Delta x_{i+k} + \frac{\Delta x_{i+k}}{2} \quad (14)$$

and the minimum composition is calculated as

$$C_{i+k} = \frac{\pi d^2 \times 100 \times P_l}{4 \times \Delta x_{i+k} \times P_d \times P_l}$$

Therefore,

Error in length = actual length- calculated length

$= L - L_i$

Error in composition = desired minimum composition - calculated minimum composition

$= C_{min} - C_{i+k}$

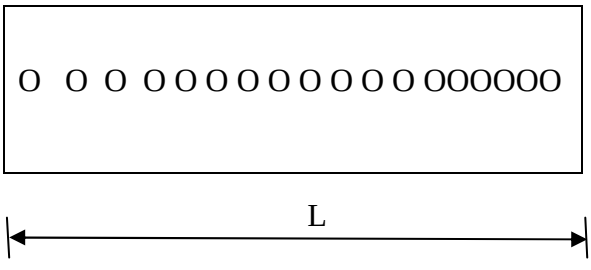

Fig. 5. Holes representing maximum to minimum composition variation

From the numerical model, considering the different electrode diameters (hole diameters) such that the maximum composition can be defined for the fixed pin diameter. In this study FSP tool of pin diameter 6.2 mm is used, the C_{max} values are calculated for different electrode diameters as shown in Table 1.

For a fixed tool pin diameter, variation in hole diameters (electrode diameters) lead to the variation in maximum compositions and this variation is shown in Fig. 6.

Table 1 C_{max} values for different diameters without overlap of holes

Diameter (mm)	1.5	1.2	1	0.8	0.6	0.4
C_{max} (%)	19.001	15.201	12.667	10.134	7.6	5.067

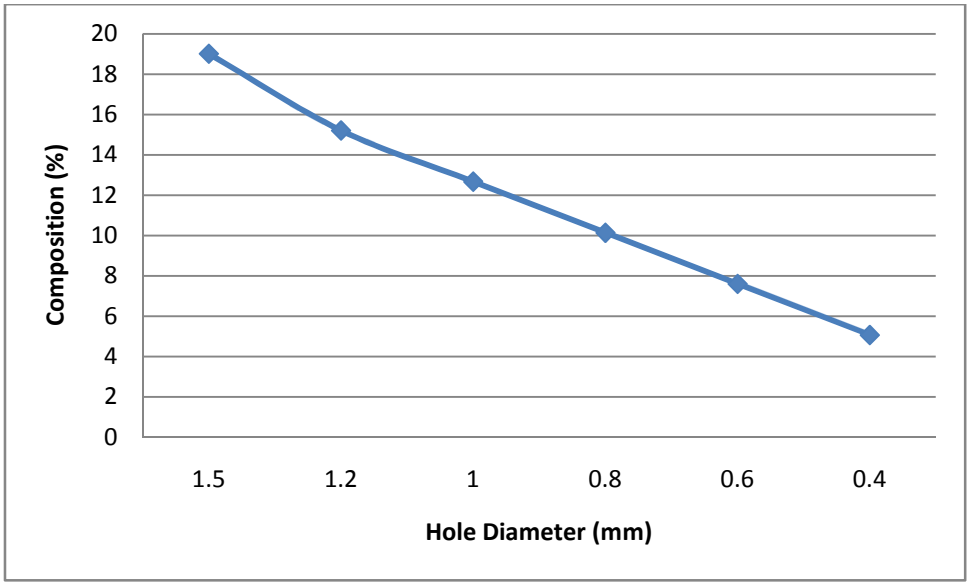

Fig. 6. C_{max} vs. Hole diameter

For a fixed maximum composition (C_{max}) values, the errors in length and composition can be determined by varying minimum composition (C_{min}) values as shown in Figures. 7 and 8 respectively.

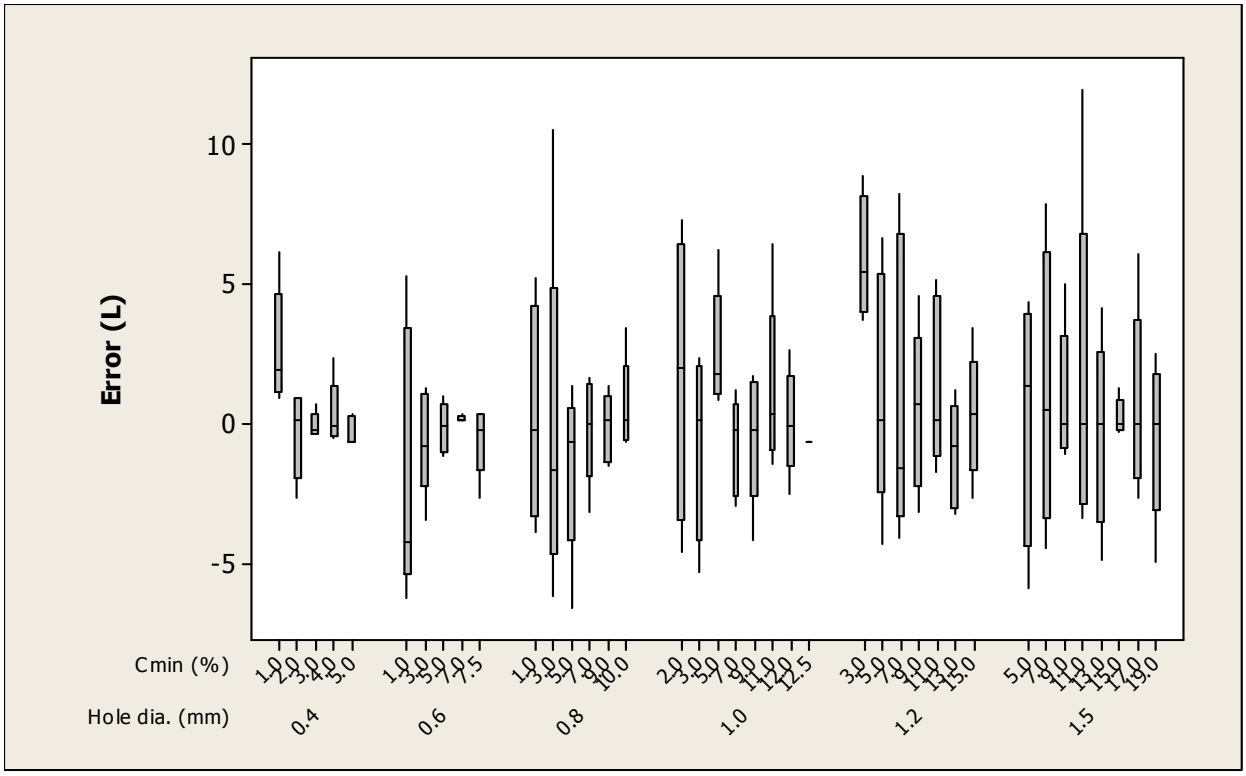

Fig. 7. Error in Length vs. C_{min}, Hole diameter

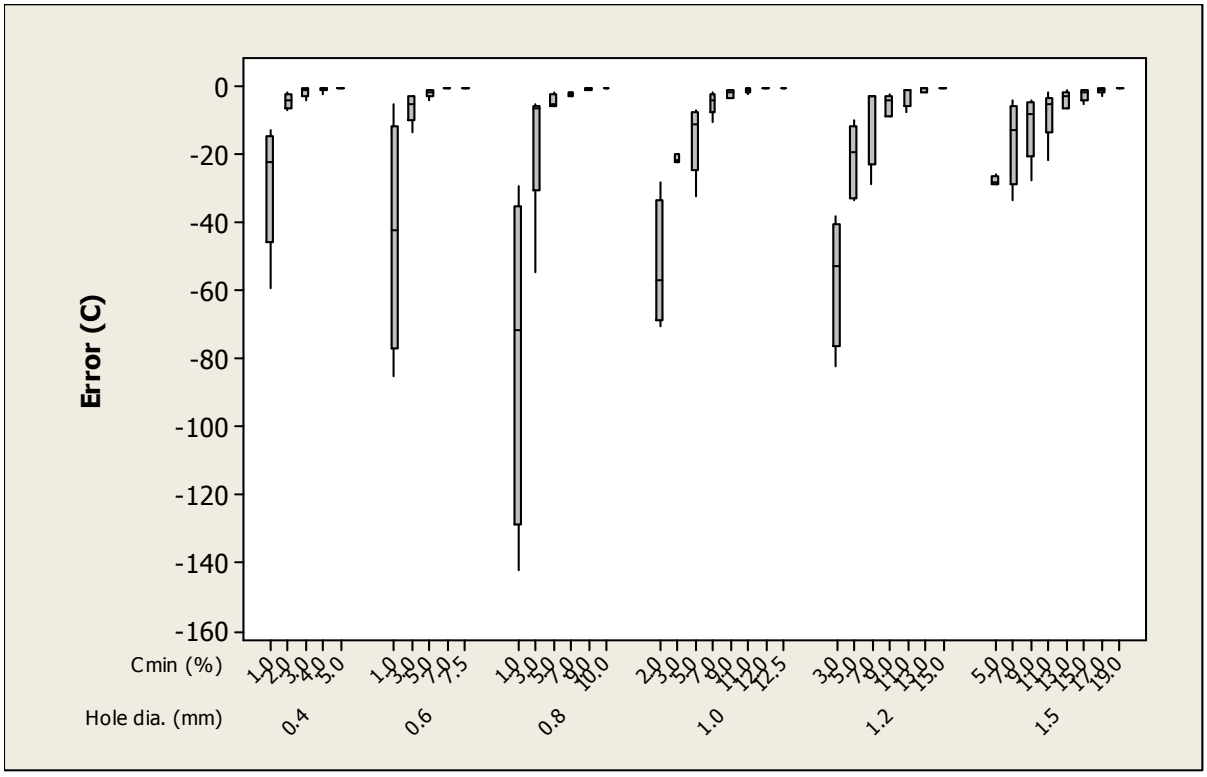

Fig. 8. Error in composition vs. C_{min}, Hole diameter

Chapter - 4

Materials and Experimental Method

The present study is carried out on commercially pure aluminium material. Vertical milling machine with FSP tool inserted is used to carry out the FSP experiments. The following section gives details about the materials, tool used and experimental procedure used for FSP process.

4.1 Materials

In this study, 6 mm thick plate of commercially pure aluminium was used as base material and alumina nano-particles of size (<50nm) and TiC particles of size 325 mesh were used as shown in Fig. 9. The chemical composition of the base material used is shown in Table 2. The mechanical properties of the base material used are shown in Table 3.

Table 2 Chemical composition of base material

Material	Al	Cu	Fe	Mn	Si	Zn
Commercially Pure Aluminium	98.95	0.005	0.457	0.014	0.564	0.006

Table 3 Mechanical properties of base material

Material	Plate thickness (mm)	Yield stress (MPa)	Ultimate tensile strength (Mpa)	Young's modulus (GPa)
Commercially Pure Aluminium	6	90	113.91	59.092

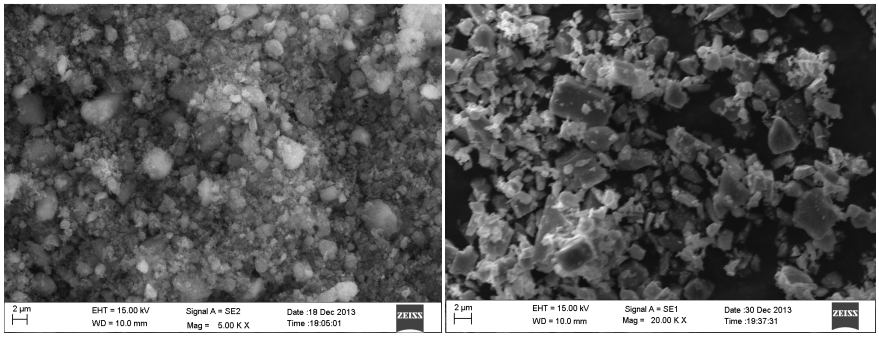

Fig. 9. SEM images of (a) Alumina and (b) TiC particles

The experiments were conducted in the CNC vertical milling machine with a FSP tool and hole EDM with a brass electrode of diameter 1 mm. The FSP tool has the following geometry and is shown in Fig. 10.

4.2 FSP tool geometry

The material used for the tool is H13 tool steel with a cylindrical pin

Pin diameter – 6.2 mm

Pin length - 5.2 mm

Shoulder diameter – 27 mm

Fig. 10. FSP tool

4.3 Sample preparation

From the numerical model in chapter 3, Considering the maximum composition (C_{max}) as 8% and the minimum composition (C_{min}) as 2%, the linear change in composition occurs over a length of 40 mm is calculated and the variation of composition with respect to the length is shown in Fig. 11. In the present study, for a fixed hole diameter of 1mm, the length of the grids Δx_i values have been primarily calculated as shown in Table 4.

Table 4 Grid lengths for different compositions

Hole no. (i)	Δx_i **(mm)**	**Composition (%)**
1	1.583	8.000
2	1.633	7.759
3	1.687	7.510
4	1.747	7.252
5	1.813	6.985
6	1.889	6.708
7	1.974	6.418
8	2.072	6.115
9	2.186	5.795
10	2.321	5.457
11	2.485	5.097
12	2.690	4.708
13	2.956	4.285
14	3.321	3.814
15	3.868	3.275
16	4.830	2.623

Therefore,

Error in length: 0.944

Error in composition: -0.263

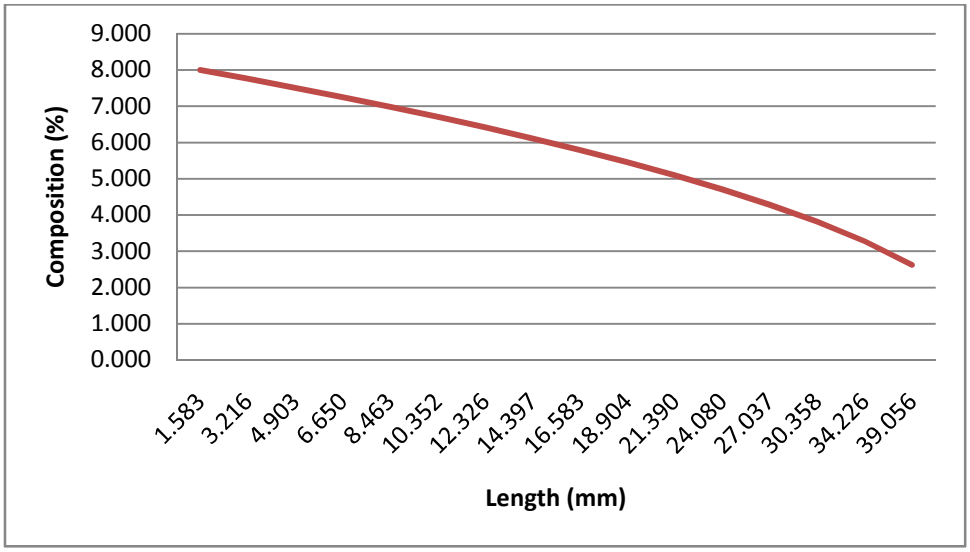

Fig. 11. Length vs. Composition

The holes have been drilled on the aluminium plate using hole electrical discharge machine with a brass electrode of diameter 1 mm with the Δx_i values calculated from the numerical model. These holes were filled with Alumina (Al_2O_3) of particle size (<50nm) and TiC particles of size 325 mesh. Hence the grid size changes in such a way that the percentage composition of reinforcement particles changes accordingly i.e. linearly. Multiple samples each have been prepared as shown in Figures. 12 and 13 in order to perform multi-pass FSP (one pass, two pass, three pass and four pass) in the same directions and in the opposite directions.

Fig. 12. Holes filled with Alumina nano-particles

Fig. 13. Holes filled with TiC particles

Friction stir processing has been carried out on the filled holes in different number of passes and in different (same and opposite) directions with the stated FSP tool geometry and the following parameters.

Spindle speed – 1000 rpm

Travel speed - 50 mm/min

Tilt angle - 0°

During FSP the localized heating is produced which rises the viscoplastic behavior at the interface of reinforcement particles and base material. Thus, joining takes place. The work piece material flow takes place from front to the back of the pin, where it is forged under shoulder pressure forming the bead.

4.4 Measurements and Tests

4.4.1 Hardness distribution

The FSPed samples are cut longitudinally at the center along the direction parallel to the surface. This is done using the wire-electrical discharge machine so that the hardness is minimally altered by the cutting process. The hardness survey was done at the center of the stirred samples along the longitudinal section using a Vickers hardness tester with a load of 100 kgf.

4.4.2 Strain measurement

The specimens are produced for DIC testing as shown in Fig. 14. The Digital Image Correlation (DIC) testing is carried out using a 100 kN capacity MTS UTM. The DIC testing is based on recording a series of images of the specimen during the deformation with digital cameras and calculating the surface displacements from these images. To apply this method, the specimen needs to be prepared by the application of a random dot pattern (speckle pattern) on its surface. Titanium white paint (acrylic aerosol paint) is sprayed on the surface of the specimen to provide a base for the black color speckle and it is allowed to dry for half an hour. After drying the white paint, random speckle pattern of carbon black paint (golden air brush color) is applied over the white surface with an airbrush compressor having a nozzle of 0.5 mm diameter. The speckle pattern on the specimen surface is as shown in Fig. 15.

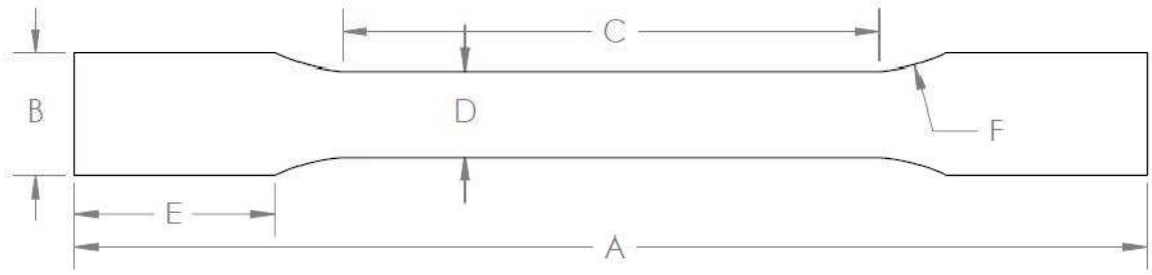

Fig. 14. DIC test sample specification

A= 100 mm, B= 10 mm, C= 32 mm, D= 6 mm, E= 30 mm, F= 6 mm, Thickness =6 mm

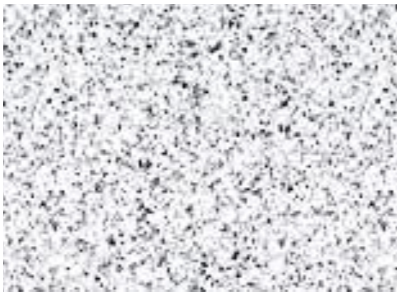

Fig. 15. Speckle pattern

Chapter 5

Results and Discussion

The results obtained for the multi-pass FSP is discussed. The variation in mechanical properties such as hardness, Young's modulus of FGM is presented. SEM micrographs are presented to support the findings.

5.1 Surface Appearance

The multi-pass FSP (two pass and three pass) provides a good material flow and joint with continuous rings than single FSP in both the cases with and without reinforcement particles. The outlook of these materials shows information about the processing quality as shown in Fig. 16, 17. Since FSP joints are accompanied by the defects like tunnel defect, cracks etc. The three pass stir joints provide defect free welds than the single pass and two pass stir as shown in Fig. 18.

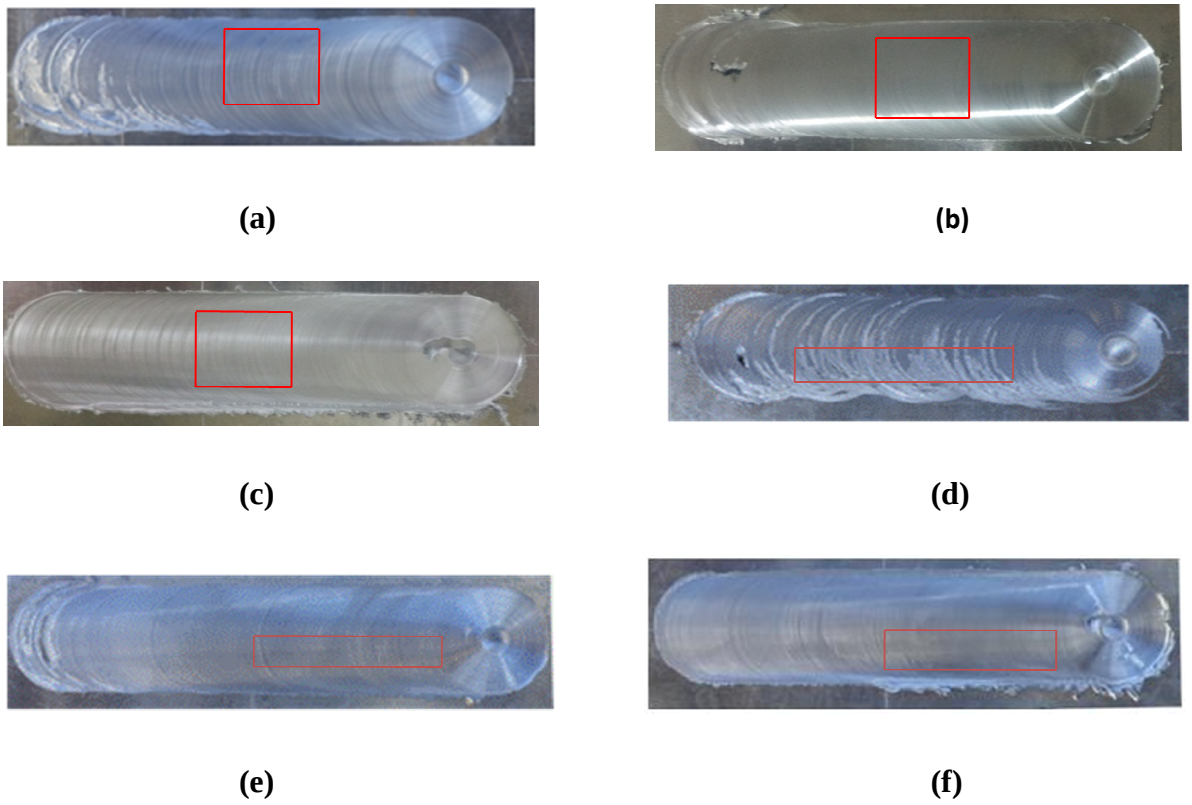

Fig. 16. Macroscopic pictures of multi-pass stirred samples (a) Plain single pass FSP (b) Plain two pass FSP (c) Plain three pass FSP (d) Alumina single pass FSP (e) Alumina two pass FSP and (f) Alumina three pass FSP

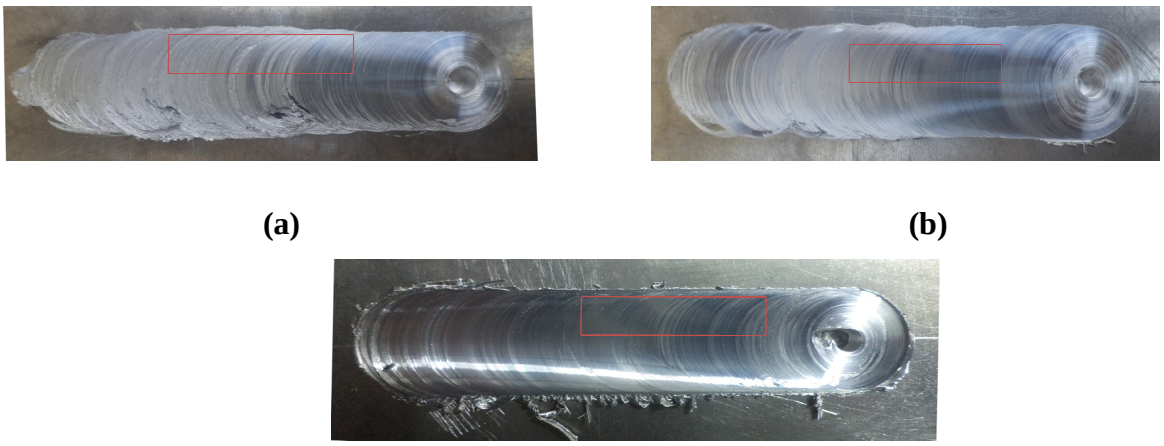

Fig. 17. Macroscopic pictures of multi-pass stirred samples (a) TiC single pass FSP (b) TiC two pass FSP (c) TiC three pass FSP

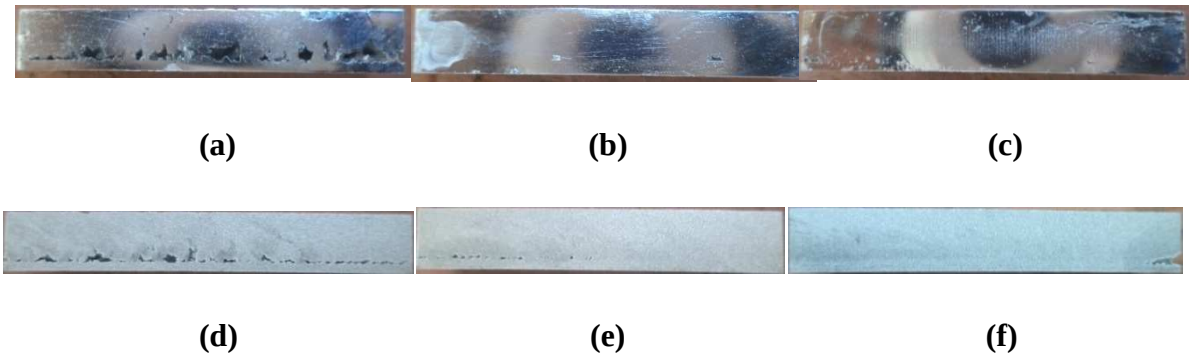

Fig. 18. Cross sectional view of multi-pass stirred samples (a) Alumina single pass (b) Alumina two pass (c) Alumina three pass (d) TiC single pass (e) TiC two pass (f) TiC three pass

5.2 Microstructure

SEM images are taken for the single pass, two pass, three pass alumina stirred and three pass TiC stirred specimens at the longitudinal section (center) i.e. at the nugget zone. The microstructures of alumina particles with one pass, two pass and three pass FSP are shown in Figures. 19, 20 and 21 respectively. The microstructures of TiC particles with three pass FSP are shown in Fig. 22.

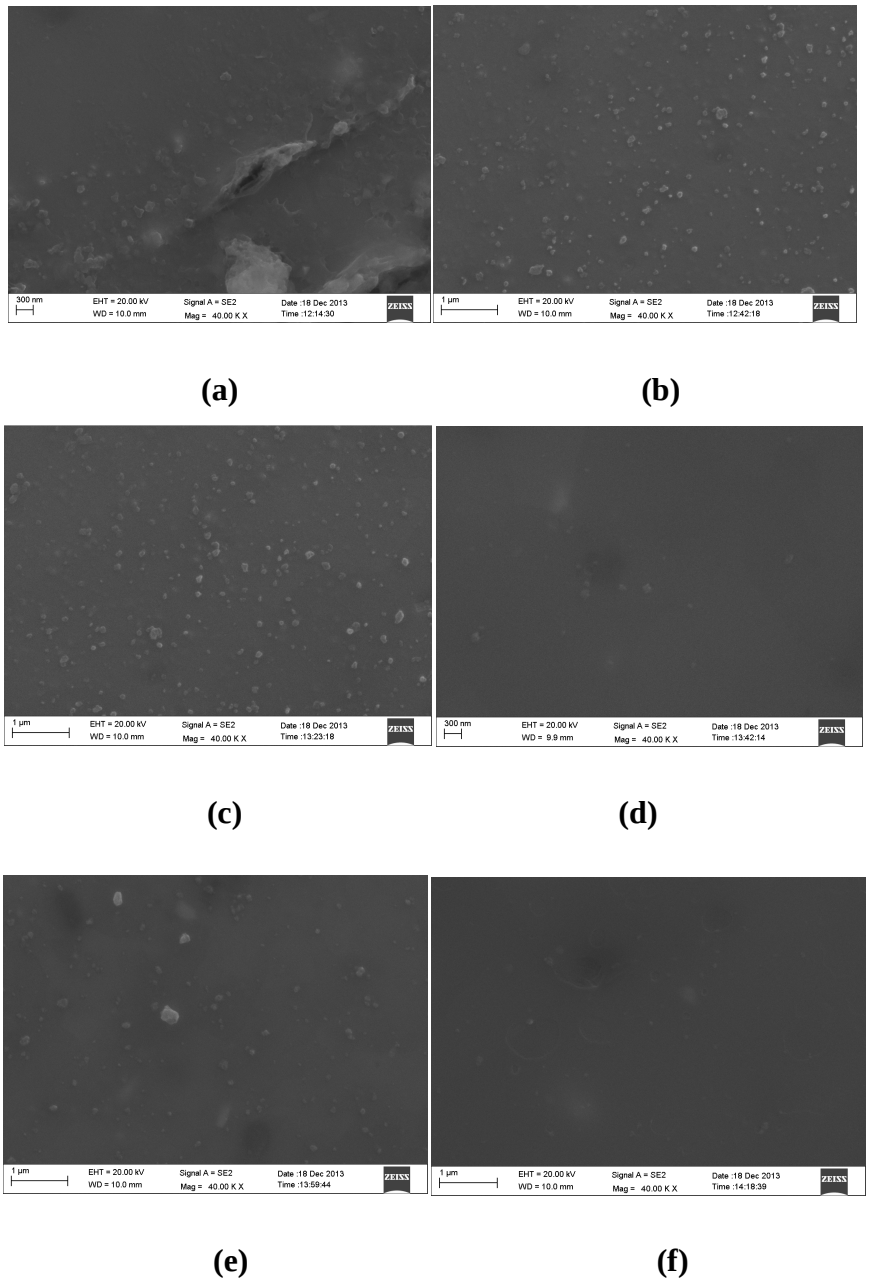

Fig. 19. SEM micrographs of alumina single pass friction stir processed zone on cross-sections parallel to tool traverse direction at a distance of (a) 0.5 mm (b) 7.1 m (c) 13.7 mm (d) 20.3 mm (e) 26.9 mm and (f) 33.5 mm from the C_{max} end

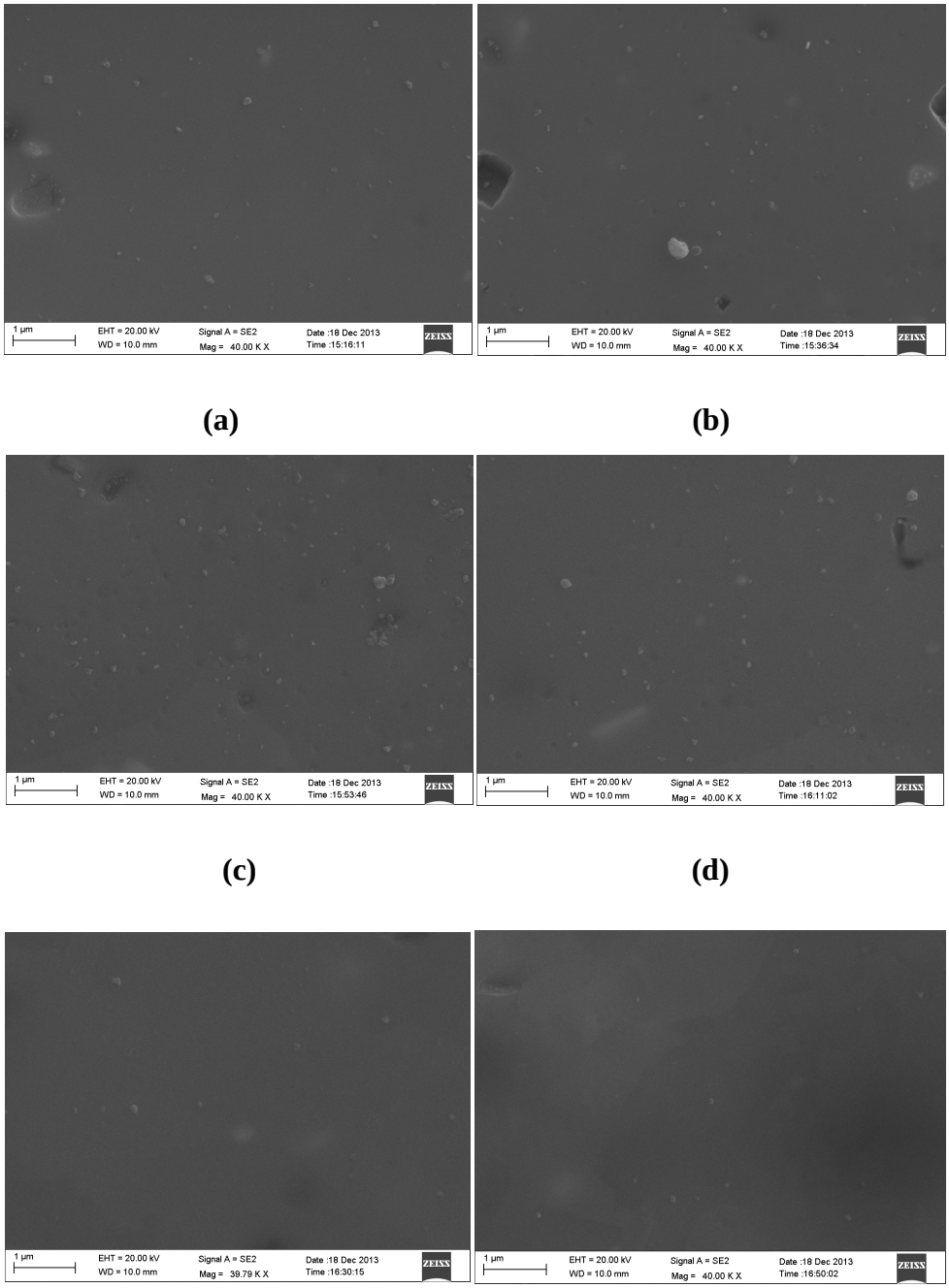

Fig. 20. SEM micrographs of alumina two pass friction stir processed zone on cross-sections parallel to tool traverse direction at a distance of (a) 0.5 mm (b) 7.1 mm (c) 13.7 mm (d) 20.3 mm (e) 26.9 mm and (f) 33.5 mm from the C_{max} end

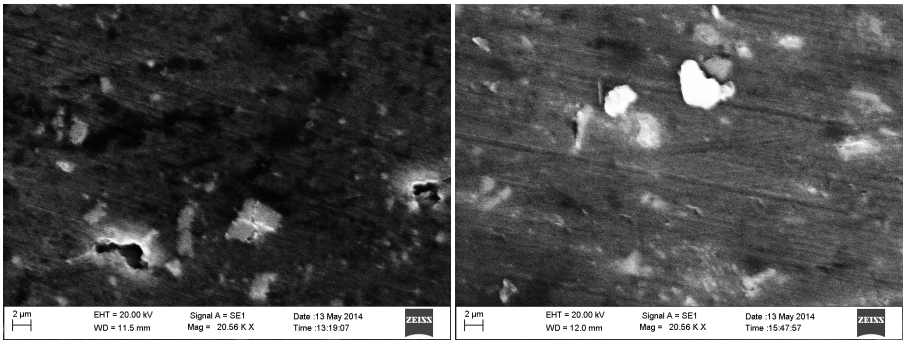

(a) **(b)**

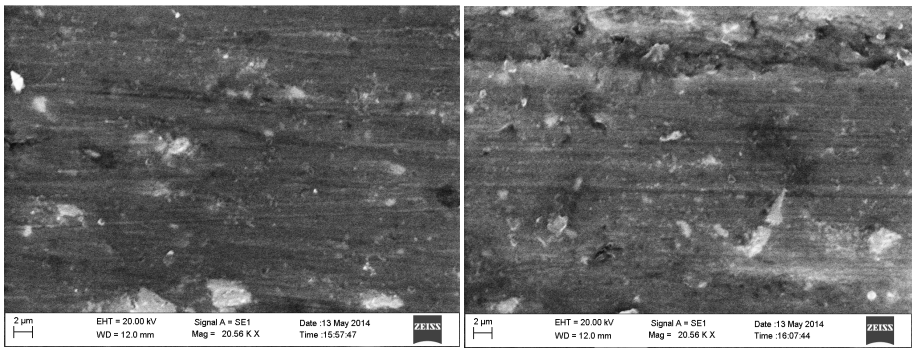

(c) **(d)**

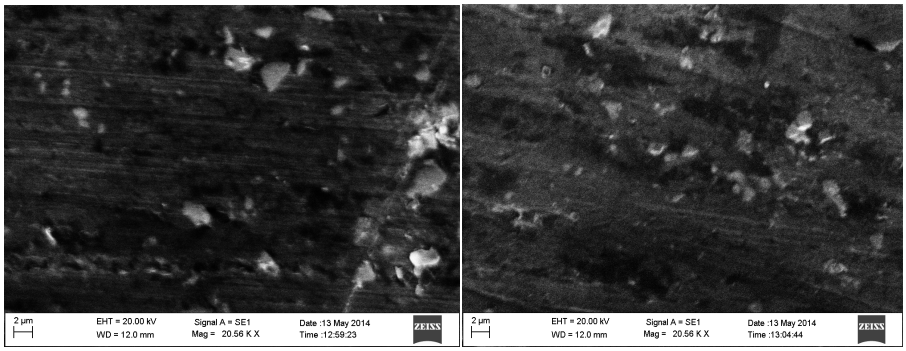

(e) **(f)**

Fig. 21. SEM micrographs of alumina three pass friction stir processed zone on cross-sections parallel to tool traverse direction at a distance of (a) 0.5 mm (b) 7.1 mm (c) 13.7 mm (d) 20.3 mm (e) 26.9 mm and (f) 33.5 mm from the C_{max} end.

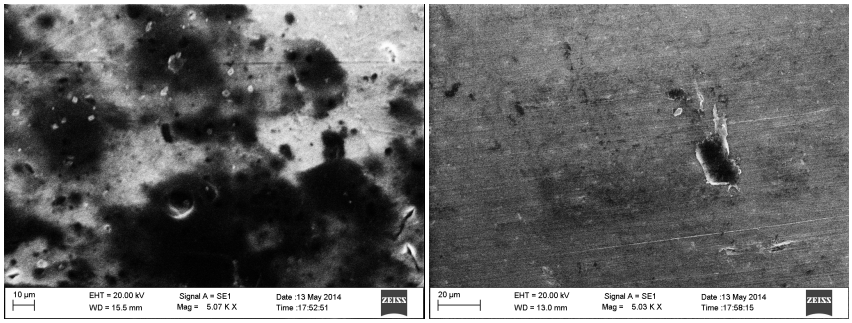

(a) **(b)**

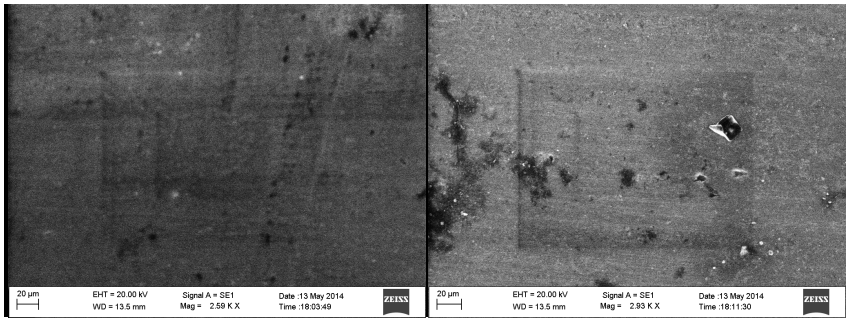

(c) **(d)**

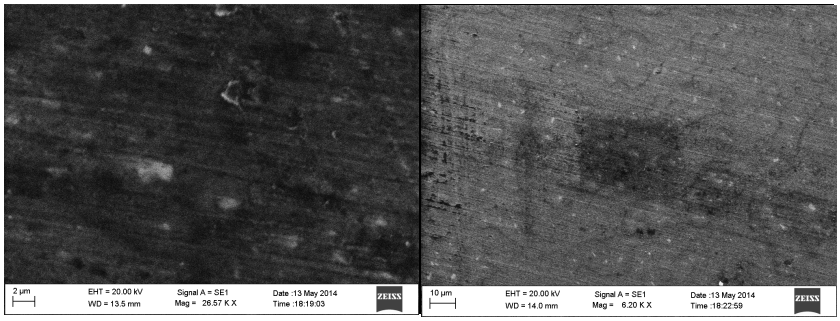

(e) **(f)**

Fig. 22. SEM micrographs of three pass TiC friction stir processed zone on cross-sections parallel to tool traverse direction at a distance of (a) 0.5 mm (b) 7.1 mm (c) 13.7 mm (d) 20.3 mm (e) 26.9 mm and (f) 33.5 mm from the C_{max} end

The microstructure characterization of all the four FGMs revealed in common, the presence of reinforcement particles. The particles can also found to decrease in number density from C_{max} to the C_{min} side. However the gradual decrease is observed in single and two pass friction stirred samples.

5.3 Hardness

The hardness survey along the longitudinal direction of the stirred samples was done using a Vickers hardness tester with a load of 100 kgf. The hardness of the pure aluminium is 35 HV. It was observed from the hardness profile of FSPed samples in the same directions

along the longitudinal section from C_{max} side that hardness values are decreasing for both alumina and TiC particles to the $C_{min\ side}$ as shown in Figures. 23 and 24.

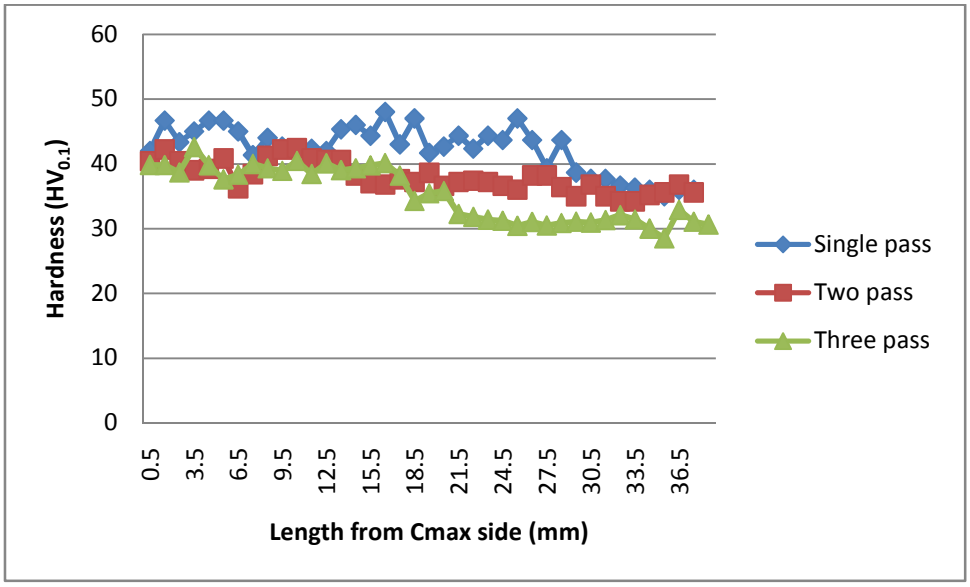

Fig. 23. Hardness profile at the longitudinal center section of one pass, two pass, three pass in the same directions of alumina stirred specimens

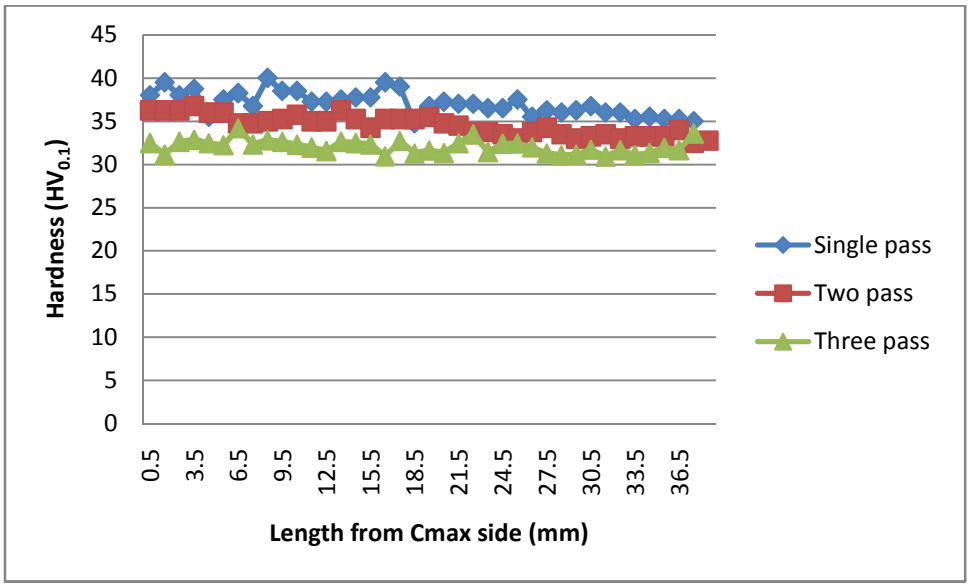

Fig. 24. Hardness profile at the longitudinal center section of one pass, two pass, three pass in the same directions of TiC stirred specimens

Decrease of hardness values in all the cases (one pass, two pass, three pass) with particles of alumina and TiC along the longitudinal section at center from C_{max} side is observed whereas a gradual decrease is observed in two pass stirred graded material.

The hardness survey along the longitudinal direction (center) for the samples of the two pass stirred in opposite direction, three pass stirred in opposite directions and four pass stirred in opposite directions was performed. An irregular trend in decrease in the hardness values is observed from the hardness profiles as shown in Fig. 25.

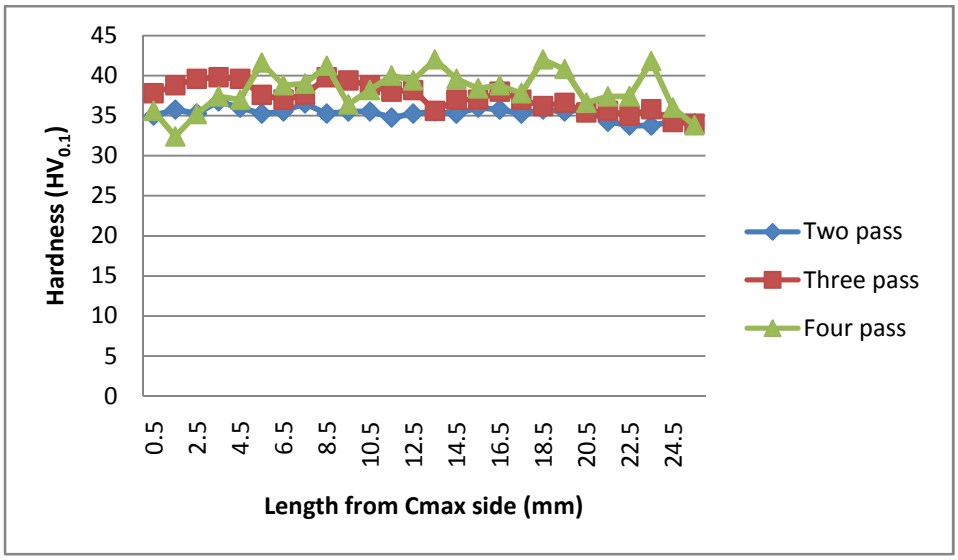

Fig. 25. Hardness profile at the longitudinal center section of two pass, three pass, four pass in opposite directions of TiC stirred specimens

5.4 Strain measurement

The multi-pass FGM specimens at center were tested for surface strain measurements using the DIC technique and found the localized strain changes. The local zone has been selected for every 2 mm as shown in Fig. 26 to determine the localized properties. The strain distributions of the FGMs are shown in Fig. 27. Since this technique starts with an image before loading (reference image) and then a series of images are taken during the loading process (deformed images). All the deformed images show a different random dot pattern relative to reference image. With commercially available software, displacement and strain distribution map has been be extracted. Hence the localized mechanical properties at every 2 mm along the length were extracted using this technique and the Young's modulus values at every 2 mm for three pass advancing side, three pass retreating side and four pass advancing side of the specimens are shown in Figures. 28, 29 and 30.

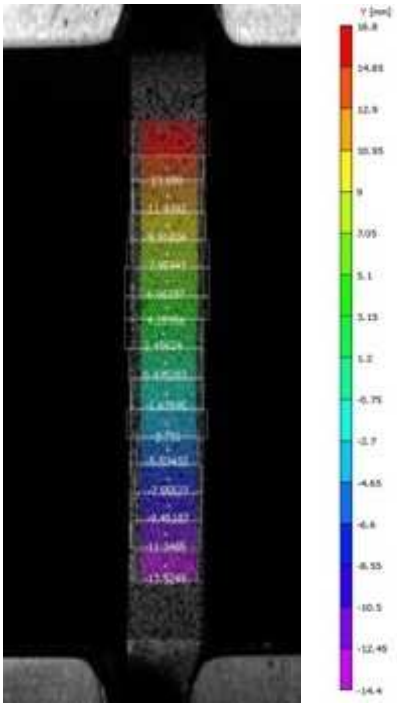

Fig. 26. Local zone selection

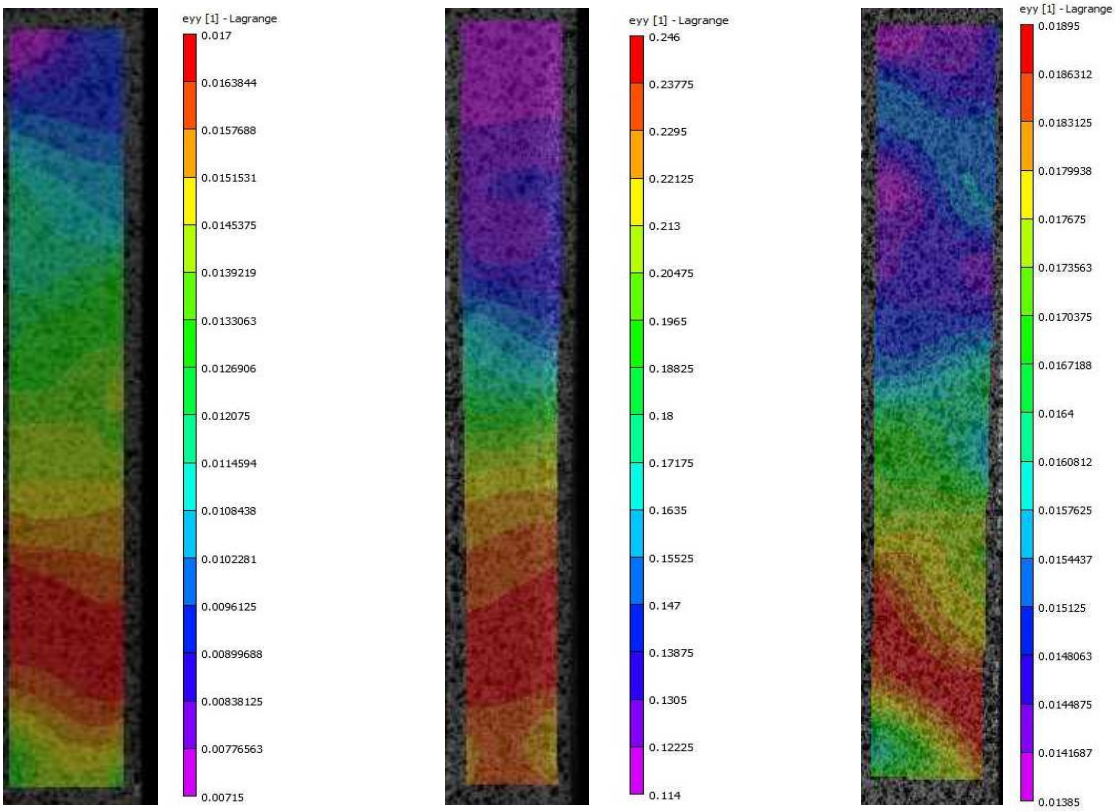

(a) **(b)** **(c)**

Fig. 27. Strain distributions of (a) three pass advancing side at Load 2kN (b) three pass retreating side at load 3.7kN (c) four pass advancing side at 2.3kN from DIC

The Young's modulus E values for every 2 mm was found using the stress-strain values from the DIC and decrease in the E values at every 2 mm is observed as shown in Fig. 28. Although some irregular variation is observed in three pass advancing side, it is possible to see a progressive gradient in properties at the advancing side whereas in three pass retreating side, an irregular decrease in the E values at every 2 mm is observed as shown in Fig. 29.

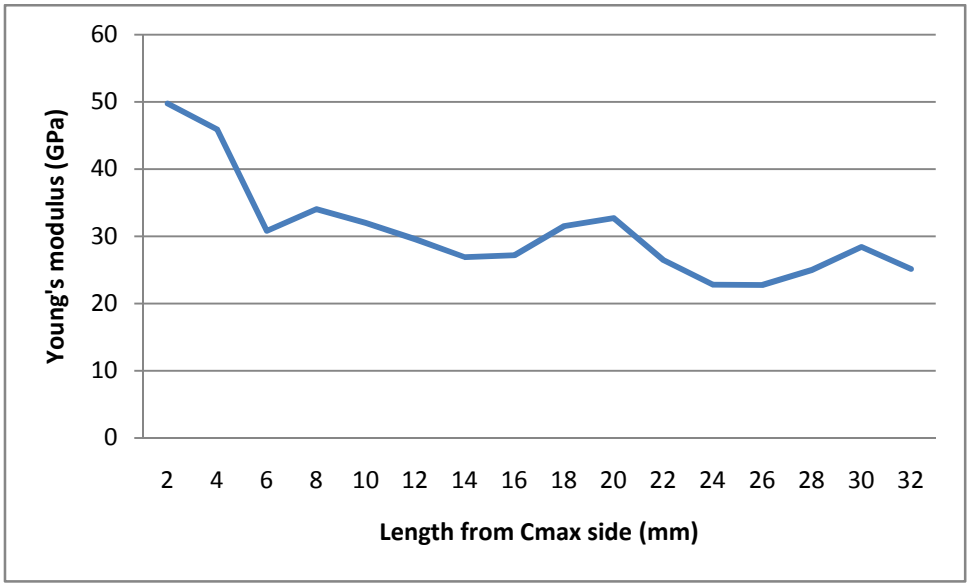

Fig. 28. E values for every 2 mm length of three pass FGM (advancing side-center)

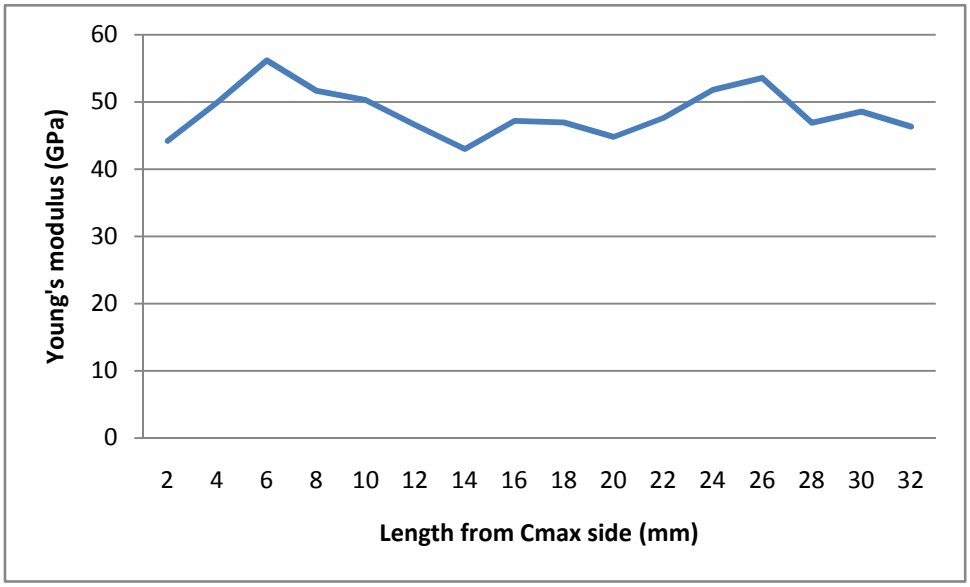

Fig. 29. E values for every 2 mm length of three pass FGM (retreating side-center)

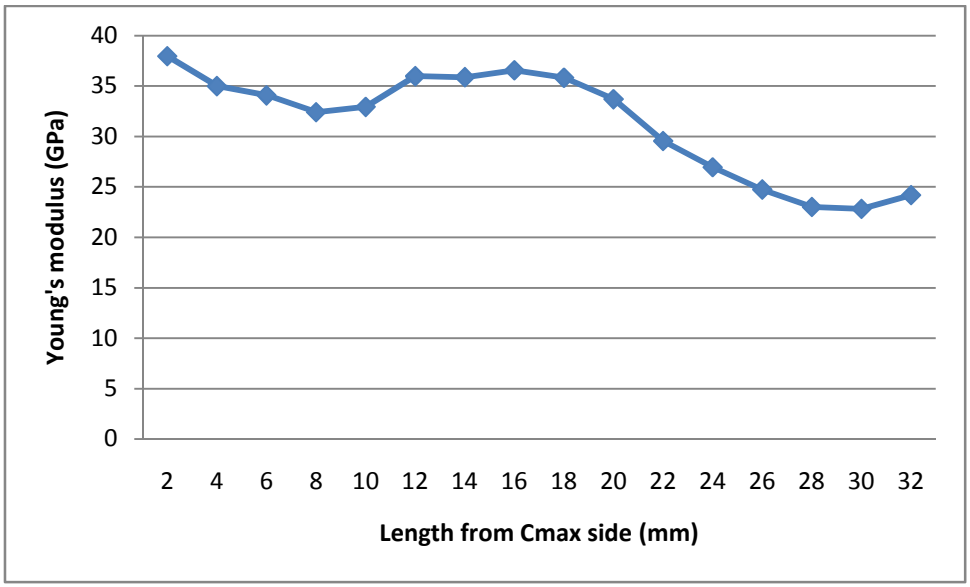

Fig. 30. E values for every 2 mm of four pass in opp. dir FGM (advancing side-center)

The Young's modulus E values for every 2 mm of four pass FSP in opposite directions at the center of advancing side sample was found using the stress-strain values from the DIC and decrease in the E values at every 2 mm is observed as shown in Fig. 30.

Chapter – 6

Conclusions and Future scope

The present study of fabrication of functionally graded material through Friction Stir Processing (FSP) is an attempt in order to overcome the control over the composition. Holes were drilled on an aluminium plate and filled with reinforcement particles. A mathematical model for positioning of holes has been developed in order to acquire the maximum to minimum composition of reinforcement particles over a given length. Multi-pass FSP has been carried out in the same directions and in opposite directions.

6.1 Conclusions

1. A numerical model for 1-dimensional functionally graded material with a linear change in composition of reinforcement particles under different conditions has been developed.
2. Three pass FSP samples results in good material flow with continuous rings than the single pass and two pass FSP samples. The three pass stir sample provides defect free joints than the single pass and two pass stir samples.
3. Decrease of hardness values in all the cases (one pass, two pass, three pass in same direction) with alumina and TiC particles along the longitudinal section at center from C_{max} side to C_{min} side is observed whereas a gradual decrease is observed in two pass stirred graded composite material.
4. The localized properties of the FGM composites was extracted using DIC technique which shows the decrease of Young's modulus values at every 2 mm from the C_{max} side.

6.2 Future scope

1. The mathematical model can be extended to parabolic change in composition of 1-D functionally graded material and linear and parabolic change in composition of 2-D and 3-D functionally graded material composites.
2. The effect of multi-pass stir can be studied further with different process parameters by varying tool spindle speed and traverse speed.
3. The effect of pin profile and shoulder diameter i.e. tool geometry can also be studied.

References

1. Mishra R.S., Ma Z.Y., “Friction stir welding and processing”, Materials Science and Engineering, R 50 (1-2), (2005), 1-78.
2. Mishra R.S., Ma Z.Y., Charit I., “Friction stir processing: a novel technique for fabrication of surface composite”, Materials Science and Engineering, A 341, (2003), 307-310.
3. Mahamood R.M., Esther T. Akinlabi Member, IAENG, Shukla M. and Pityana S., "Functionally graded material: An overview", Proceedings of the World Congress on Engineering 2012 Vol III , WCE 2012, July 4 - 6, 2012, London, U.K.
4. Kawasaki A., Cherradi N., Gasik M., “Worldwide trends in functional gradient material research and development”, Composites Engineering, Vol. 4, No. 8, (1994), 883-894.
5. Zhu J., Lai Z., Yin Z., Jeon J., Lee S., “Fabrication of ZrO_2–NiCr functionally graded material (FGM) by powder metallurgy”, Materials Chemistry and Physics, Vol. 68, (2001), 130-135.
6. Jin G., Takeuchi M., Honda S., Nishikawa T., Hideo Awaji H., “Properties of multilayered Mullite/Mo functionally graded material by powder metallurgy processing”, Materials Chemistry and Physics, Vol. 89, (2005), 238-243.
7. Zhang G., Guo Q., Li X., Zhang H., Song Y., Shi J., Liu L., “Effect of number of graded layers on microstructure and properties of SiC/C functionally graded materials”, Fusion Engineering and Design, Vol. 82, (2007), 331-337.
8. Bhattacharyya M., Kumar A., Kapuria S., “Synthesis and characterization of Al/SiC and Ni/Al_2O_3 Functionally Graded Materials”, Materials Science and Engineering , Vol. 487, (2005), 524-535.
9. Lai W., Munir Z.A., McCoy B.J., Risbud S.H., “Centrifugally assisted combustion synthesis of functionally graded material”, Scripta Materialia Vol. 36(3), (1997), 331-334.
10. Watanabe V., Vamanakab N., and Fukuic V., “Control of composition gradient in a metal-ceramic functionally graded material manufactured by centrifugal method”, Applied science and Manufacturing, Vol. 29 (5-6), (1998), 595-601.
11. Zhai Y., Liu C., Kai W., Zou M., Yong X., “Characteristics of two Al based functionally gradient composites reinforced by primary Si particles and Si in situ

Mg_2Si particles in centrifugal casting", Transactions of Nonferrous metals society of China Vol. 20, (2010) , 361-370.

12. Zhang Y., Han J., Zhang X., Xiaodong H., Li Z., Shanyi Du, "Rapid prototyping and combustion synthesis of TiC/Ni functionally gradient materials", Materials Science and Engineering, Vol. 299, (2001), 218-224.
13. Jiang H., Wang X., Yu Cheng-long, Lian-juan S. and Shuang-shuang D., "Preparation of glass-alumina functionally gradient materials by rapid prototyping technology", Key Engineering Materials Vol.368-372, (2008), 1828-1830.
14. Kawase M., Tago T., Kurosawa M., Utsumi H., Hashimoto K., "Chemical vapor infiltration and deposition to produce a silicon carbide carbon functionally gradient material", Chemical Engineering Science, Vol. 54, (1999), 3327-3334.
15. Gandraa J., Mirandaa R., Vilac P., Velhinhod A., Pamies Teixeiraa J., "Functionally graded materials produced by friction stir processing", Journal of Materials Processing Technology, Vol. 211, (2011), 1659– 1668.
16. Kwon Yong-jai., Shim seong-beom., Park dong-hwan., "Friction stir welding of 5052 aluminium alloy plates", Transactions of Nonferrous Metals Society of China, Vol. 19, (2009), 23-27.
17. Uygur I., "Influence of shoulder diameter on mechanical response and microstructure of friction stir welded 1050 Al-alloy", Archives of metallurgy and materials, Vol. 57 (1), (2012), 53-60.
18. Palanivel R., Koshy Mathews P., Murugan N., Dinaharan I., "Effect of tool rotational speed and pin profile on microstructure and tensile strength of dissimilar friction stir welded AA5083-H111 and AA6351-T6 aluminium alloys", Materials and Design, Vol 40, (2012), 7-16.